DAFNE

A **D**ecision-**A**nalytic **F**ramework to explore the
water-energy-food **NE**xus in complex and transboundary
water resources systems of fast growing developing countries

EXPOSURE SPACE AND FAILURE CONDITIONS

Deliverable D5.3

August 2019

EU H2020 Project Grant No. 690268

Programme Call: Water-5-2014/2015
Project Number: 690268
Project Title: .... DAFNE

Work-Package: WP5
Deliverable #: D5.3
Deliverable Type: .... Document
Contractual Date of Delivery: 31 August 2019
Actual Date of Delivery: .... 27 November 2019
Title of Document: .... Exposure space and failure conditions
Author(s): .... POLIMI (M. Giuliani, M. Zaniolo, J. Zatarain), HWRM-ETHZ (S. Sinclair, C. Zhou, P. Burlando)

Availability:.............................. This report is internal

Document revisions		
Author	*Revision content*	*Date*
M. Giuliani, S. Sinclair	D53_v00 - Deliverable Development Plan	02/08/2019
M. Zaniolo, J. Zatarain, M. Giuliani	D53_v01 – contribution about irrigation demand scenarios	19/08/2019
S. Sinclair, C. Zhou	D53_v02 – contribution on climate scenarios and proof-reading	30/08/2019
P. Burlando	D53_v09 – final revision	27/11/2019
P. Burlando	DAFNE_D53.pdf submitted	27/11/2019

Table of Contents

List of Figures

Abbreviations

DAF: Decision Analytic Framework

OTB: Omo-Turkana basins

RCP Representative Concentration Pathway

ZRB: Zambezi river basin

1. INTRODUCTION

This deliverable concerns the preparation of the relevant data-sets for exploring the exposure space (with respect to socio-economic and climate drivers) in order to design robust pathways in deliverable D5.4. In addition, we identify thresholds on selected indicators to be evaluated in D5.4. In this short report, we describe the data-sets prepared, based on the initial experiments described in deliverable D5.2. The data-sets are stored in the DAFNE data repository.

2. GENERATION OF EXPOSURE SPACE

In deliverable D5.2 the architecture of the Decision Analytic Framework (DAF) for strategic optimization of the basin was described. The inputs to the DAF are streamflows at the nodes upstream of the basin infrastructure, and irrigation demands at the relevant agricultural district nodes in the case study basins.

In this section of the report, we describe the rationale for the procedure adopted for the perturbation of the stream flows (section 2.1), and the irrigation demands (section 2.2). In sections 3 and 0 we indicate the detail for each case study catchment Zambezi (ZRB) and Omo-Turkana (OTB) respectively.

2.1 CLIMATE CHANGE SCENARIOS

Since the exposure space of the DAF system model is directly influenced by river flows upstream of the basin infrastructure, we prepared an ensemble of flow simulations based on the climate scenarios developed in deliverable D2.2. In the OTB, our climate ensemble consists of 30 members for the period 2020-2100, and each of two Representative Concentration Pathways (RCP4.5 and RCP8.5). While for the ZRB, our climate ensemble consists of 30 members for the period 2020-2060, for a single RCP (RCP4.5). The flow simulations produced are described in section 3.1 and section 4.1 respectively.

2.2 IRRIGATION DEMAND SCENARIOS

Projected irrigation demands depend upon a number of assumptions that can be highly uncertain (e.g. the type of crop, expected cultivated area, yield and efficiency of the irrigation system in the future). Hence, relying on a single nominal projection may misrepresent the expected system's performance and could pose operational challenges in the future. Different strategies have been proposed in the literature to increase robustness against uncertainty of factors that could have a decisive impact in the decision-making process by generating plausible states of the world (e.g. Lempert, 2002; Herman et al., 2015). These states of the world are usually drawn from sampling uniformly across the upper and lower bounds of uncertain factors, expressly those whose likelihood is unknown or is difficult to quantify. This practice has been adopted in several water resources studies for vulnerability assessment under a range of hydroclimatic and socioeconomic factors (e.g., Kasprzyk et al., 2013; Herman et al., 2014; Quinn et al., 2018) and looks to be appropriate for the DAFNE case studies, due to the complex and rapidly changing regional agricultural dynamics that present a severe challenge when generating irrigation demands. Demand estimates for irrigation, for instance, can suffer unforeseen alterations due to their dependence on population growth rates and on the effects of climate change; the latter is linked to crop yields which can change unexpectedly, potentially pushing for increased water demands for crops that traditionally do not depend upon irrigation.

Following this approach, the generation of irrigation demand samples for both the ZRB and the OTB is informed by the nominal average demand projections introduced in Deliverable D2.2. The ZRB consists of three nominal scenarios: the current demands with 45% irrigation efficiency, and the planned scenarios which include current+planned+extra maize scenarios with both 45% and 67% irrigation efficiencies. Similarly, the OTB has two nominal scenarios consisting of the average demand with 45% and 67% efficiency. Starting from these nominal scenarios (3 for the ZRB and 2 for the OTB), we expand the analysis generating plausible alternative scenarios for each nominal projection (+-5% and+-10%) with the goal of providing a direct and timely assessment of how variations in irrigation demands can affect the performance of the efficient pathways illustrated in Deliverable D5.2. It is worth noting that these variations are themselves uncertain but they serve the purpose of gaining insight about the system's sensitivity to projected demands

3. EXPOSURE SPACE FOR THE ZAMBEZI RIVER BASIN

In this section we describe the data-sets prepared for analysing the exposure space in the Zambezi river basin.

3.1 CLIMATE CHANGE SCENARIOS

Because the streamflow exposure space is required at the nodes upstream of the basin infrastructure and because of high computational demand of the hydrological model developed in WP3, we decided to use the stochastically generated climate forcing to feed an established conceptual hydrological model, the HBV[1], which produced the ensemble flow simulations at the desired locations at the outlet of four sub-basins (Figure 1). As only flows were required, this allowed a more efficient generation of the streamflows representing the exposure space while maintaining an appropriate quality of the simulations. Figure 2 and Figure 3 show an example of annual precipitation and mean daily temperature for one random realisation of the simulated ensemble.

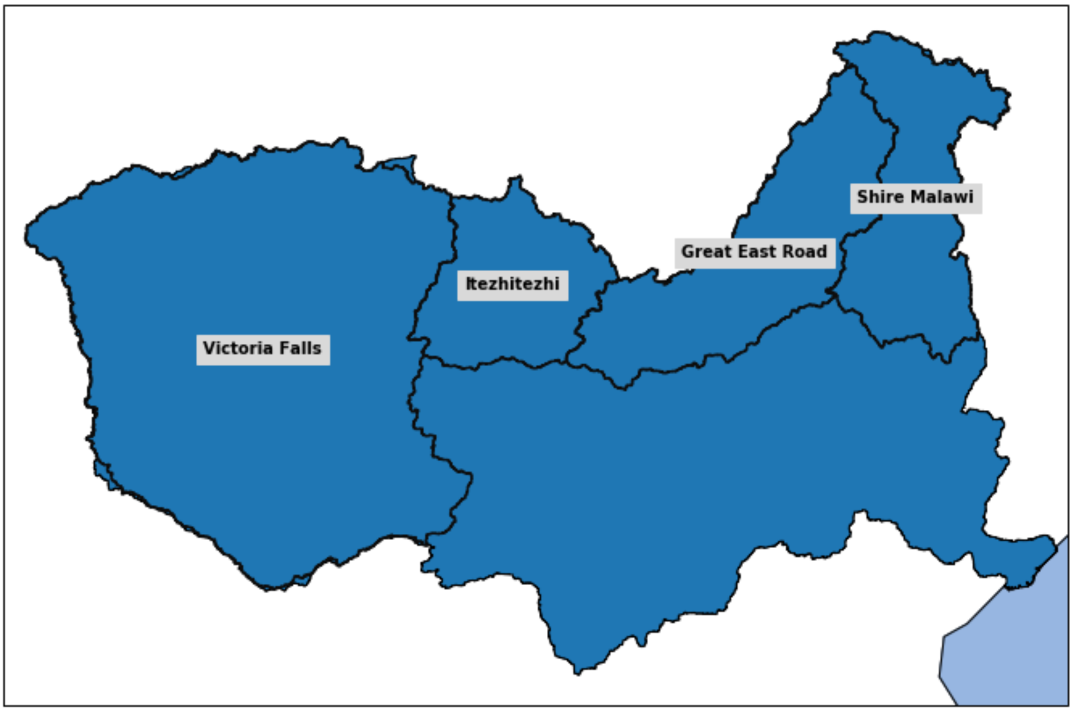

Figure 1 – Four catchments for which an HBV model was created to simulate streamflows at the nodes upstream of the basin hydropower infrastructure.

[1] https://www.smhi.se/en/research/research-departments/hydrology/hbv-1.90007

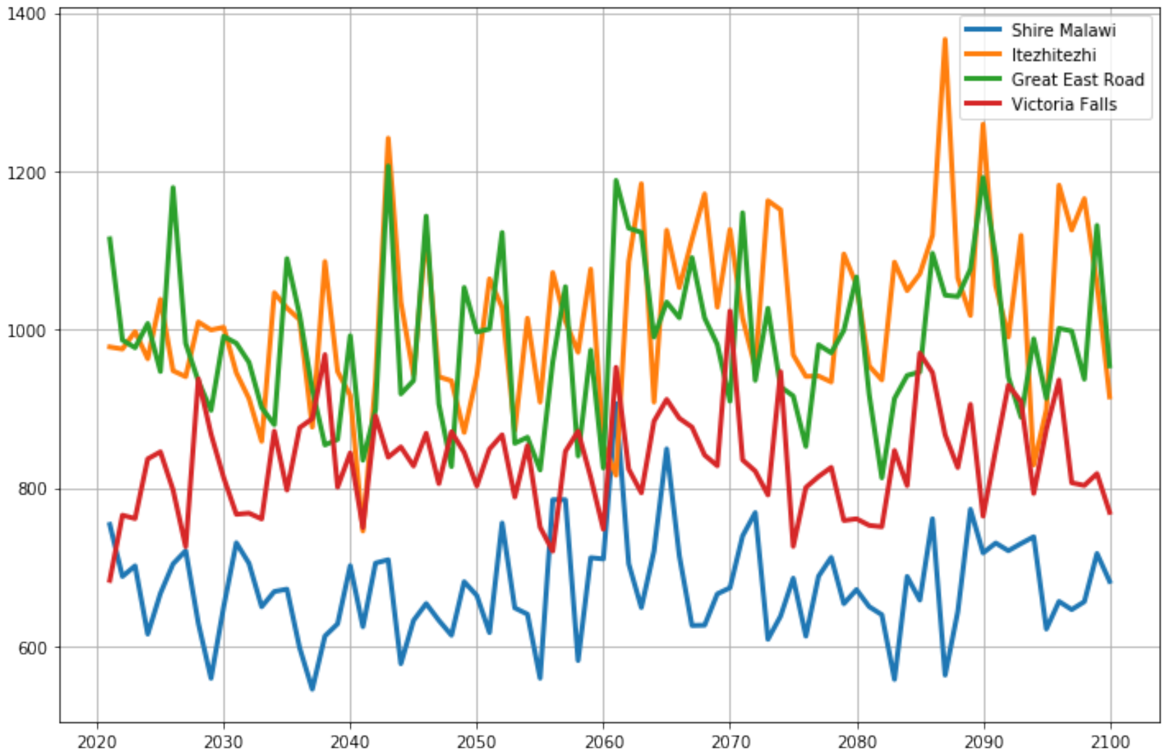

Figure 2 – Annual precipitation totals (Y-axis in mm) for a single climate realization, averaged over each sub-basin.

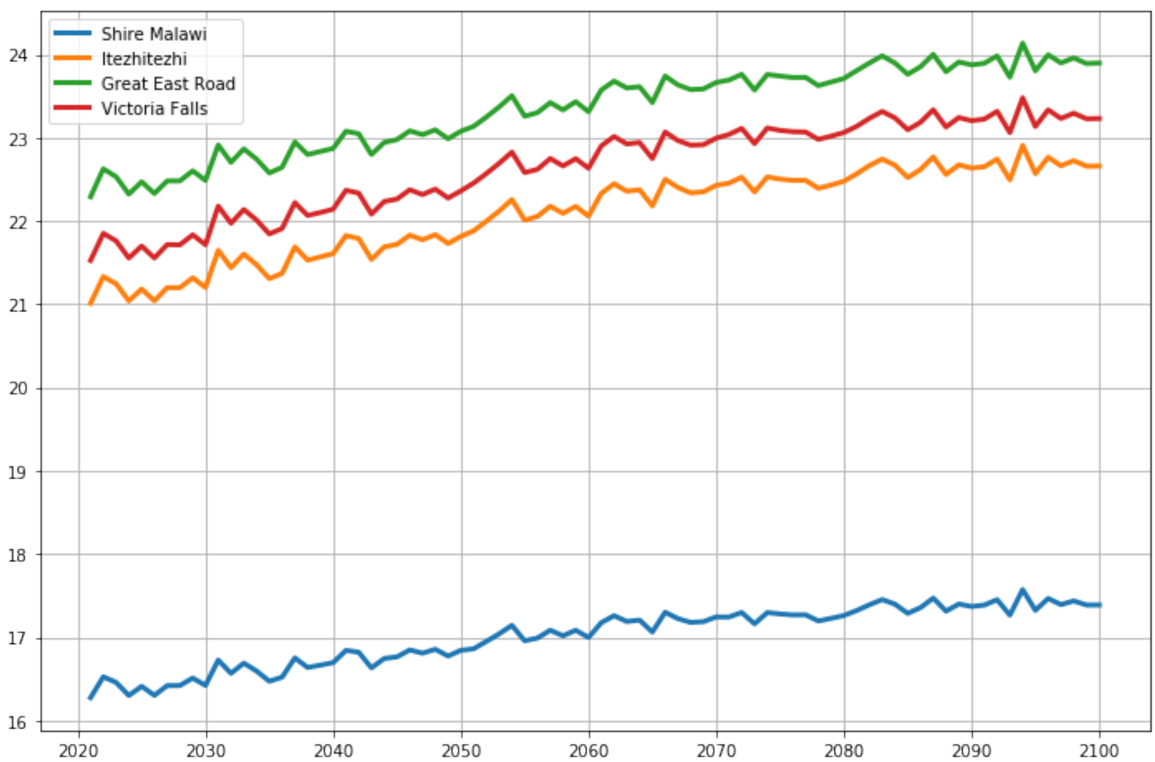

Figure 3 – Annual mean daily temperature (Y-axis in °C) for a single climate realization, averaged over each sub-basin.

3.2 IRRIGATION DEMAND SCENARIOS

The nominal irrigation demands for the Zambezi were generated through the AquaCrop model to capture the production activities of the Zambezi sub-basins as described in details in Deliverable D2.2, thereby including the impact of climate change. The projected demands result from aggregating current irrigation, planned irrigation extension and extra irrigation specifically for maize cultivation, these projections assume a 45% and 67% irrigation efficiency. Additionally, the current nominal scenario, depicted in gray in Figure 4, only includes the current irrigation schemes assuming the lower irrigation efficiency of 45%.

As observed in the projected scenarios, irrigation demands are expected to increase considerably relative to the current state, with the overall maximum of the demand that might exceed 250% of the historical values, thus potentially becoming a critical factor for the food security in the river basin. A summary of the scenarios is illustrated in Figure 5, which reports the average daily water demand under nominal (stars, bold) and synthetic (circles) scenarios: the generated scenarios appear well distributed across the vertical axis of water demands indicating a good characterization of the variable and its uncertainty.

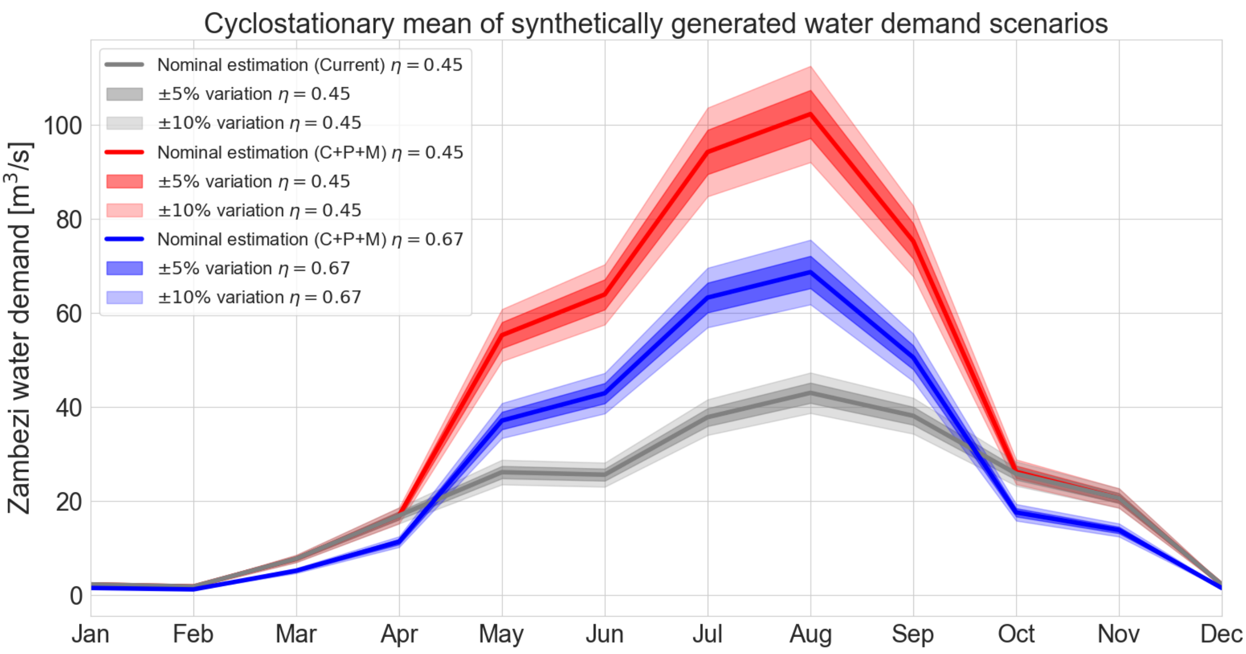

Figure 4 – Synthetic generation of water demand scenarios. Solid lines represent the cyclostationary mean of the estimated current and future water demands for the period 2020-2060, where the future water demands account for current + planned+ extra maize(C+P+M), the demands were aggregated across the 8 irrigation districts considered in the Zambezi River Basin for nominal efficiencies of 0.45 and 0.67 (red and blue line for the future demands, respectively). The shaded areas correspond to the scenarios synthetically generated by perturbing the nominal demands of ±5% (darker shade) and ±10% (lighter shade), producing a total of 12 synthetically generated scenarios on top of the 3 nominal estimations.

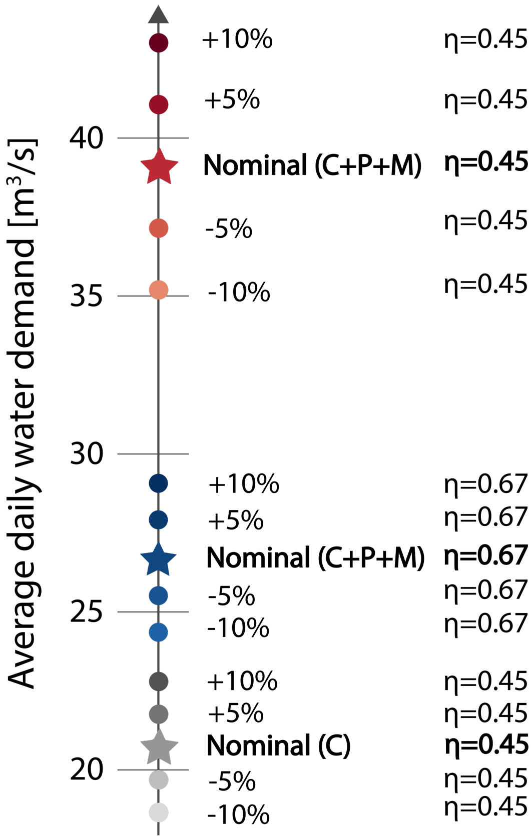

Figure 5 – A 1-dimensional representation of the mean daily water demands estimated for the future period 2020-2060 for the three nominal scenarios and the 12 synthetically generated scenarios corresponding to 0.45 and 0.67 efficiencies (red and blue points for the future scenarios respectively, and gray for the current nominal scenario(C)). Again, the future scenario considers demands for current+planned+extra maize(C+P+M). Overall, the scenarios span a daily average range of 18.6 m^3/s for the current nominal scenario with $\eta = 0.45$ and a -10% perturbation, to 43 m^3/s for the most water intensive scenario with $\eta = 0.45$ with a +10% perturbation.

4. EXPOSURE SPACE FOR THE OMO-TURKANA BASIN

In this section we describe the data-sets prepared for analysing the exposure space in the Omo-Turkana river basins (OTB).

4.1 CLIMATE CHANGE SCENARIOS

Our climate ensemble consists of 30 members for the period 2020-2100, and each of two Representative Concentration Pathways (RCP4.5 and RCP8.5). We computed the reference crop potential evaporation (ET_0) based on the Penman-Monteith formulation specified in FAO-56 (Allen et al., 1998) using the simulated climate variables for all of the realizations. Subsequently we used the ET_0 in conjunction with the downscaled precipitation simulations to produce an equivalent ensemble of 30 daily streamflow sequences for each of the two RCPs using the TOPKAPI-ETH model.

Figure 6 and Figure 7 show the median change of precipitation and reference evapotranspiration for the RCP 4.5 and RCP 8.5 respectively. Figure 8 to Figure 10 show the median changes of streamflow at the points of interest over the simulation horizon for the two RCPs 4.5 and 8.5.

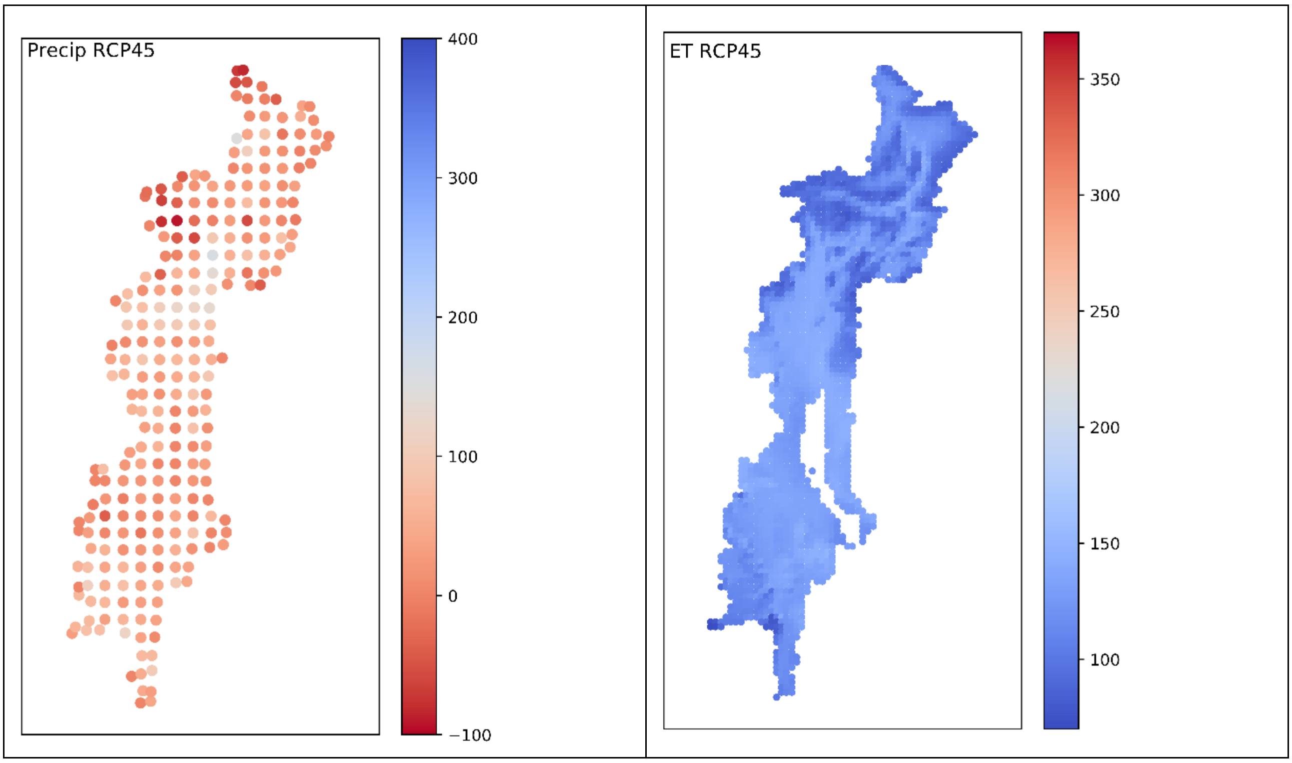

Figure 6 – Absolute change in precipitation and potential ET_0 (mm) between present and late century – RCP4.5.

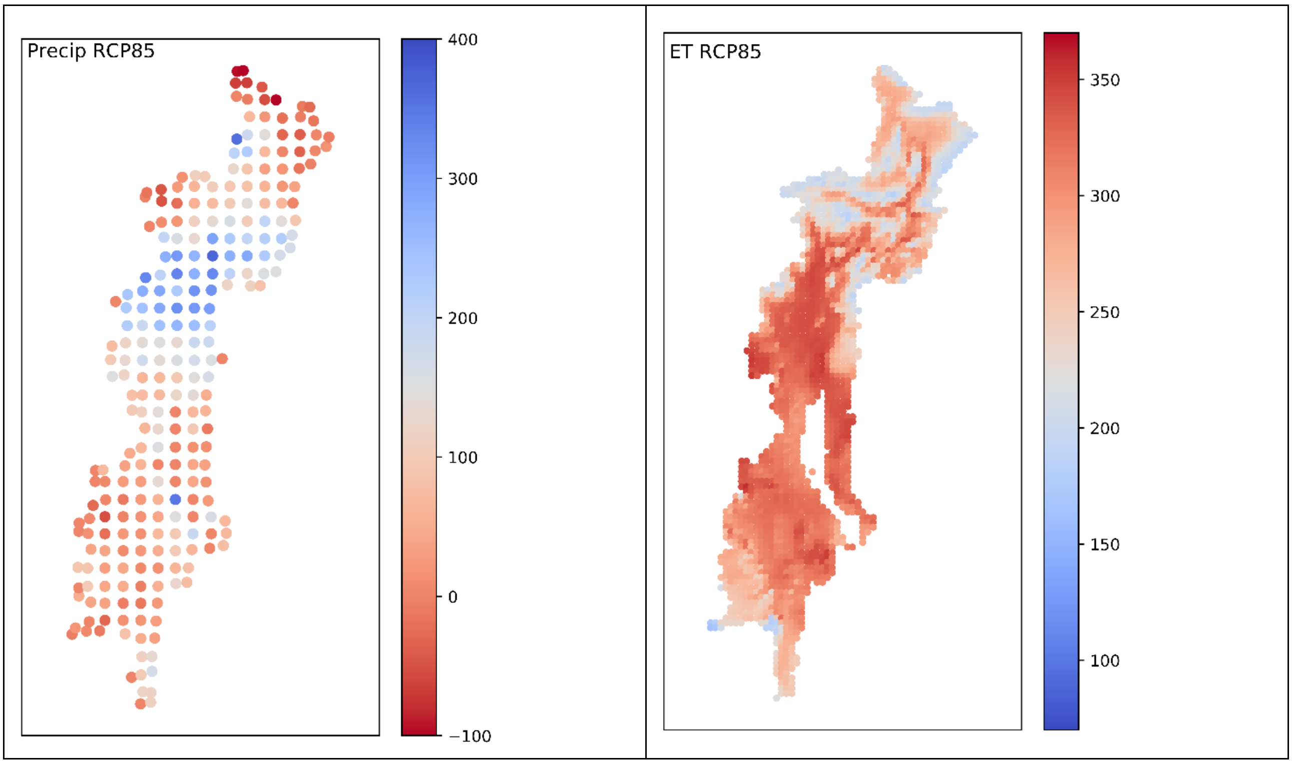

Figure 7 – Absolute change in precipitation and potential ET_0 (mm) between present and late century – RCP8.5.

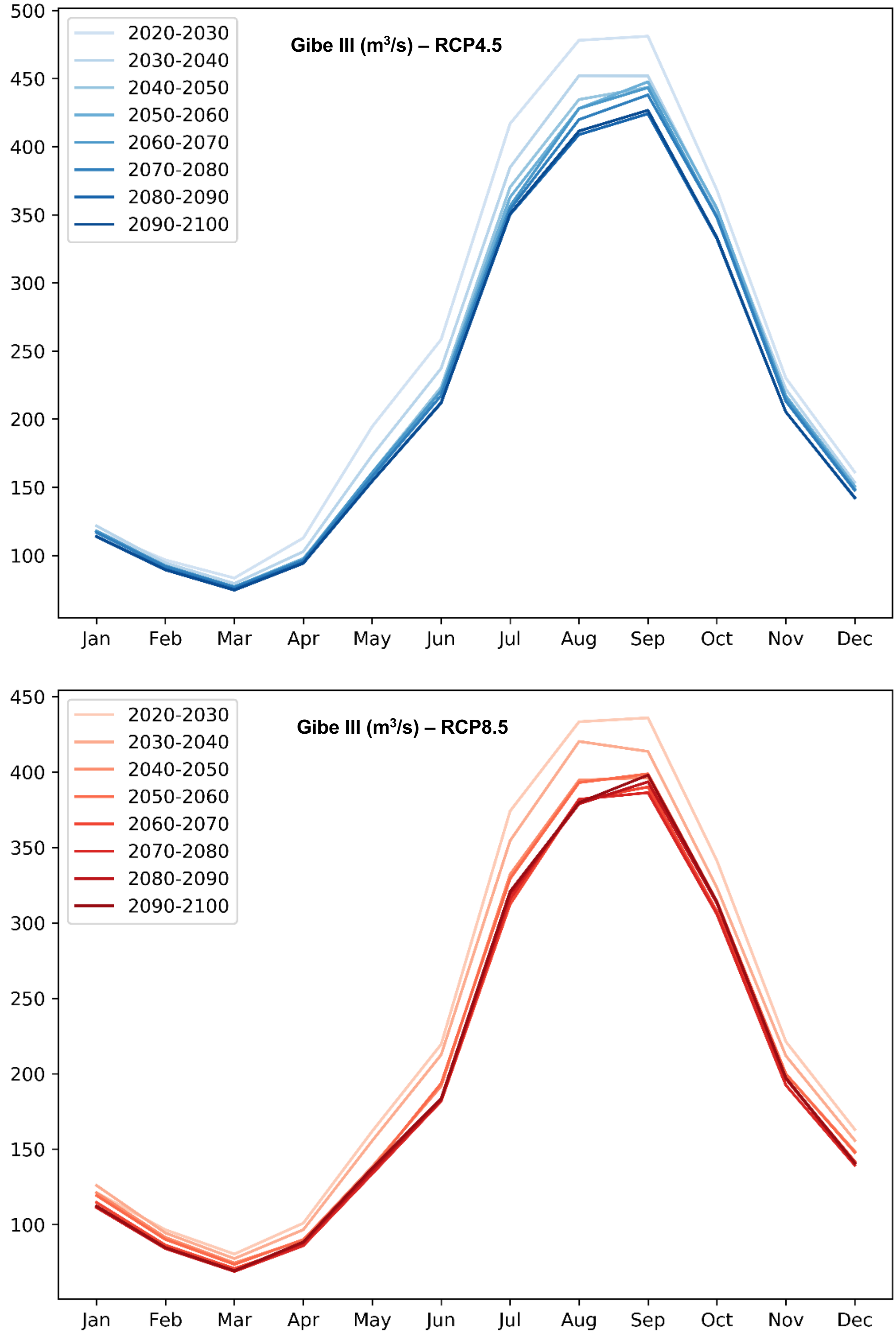

Figure 8 – Seasonal streamflow distributions after Gibe III (m3/s) for RCP4.5 and RCP8.5 climate forcings (Northern Omo). Both cases show a trend towards lower flows at the end of the century consistent with the relatively small change in precipitation relative to the increase in potential evaporation between present and end of century climate – the greater increase in evaporation for RCP8.5 results in generally lower streamflow compared with RCP4.5 (see Figure 6 and Figure 7).

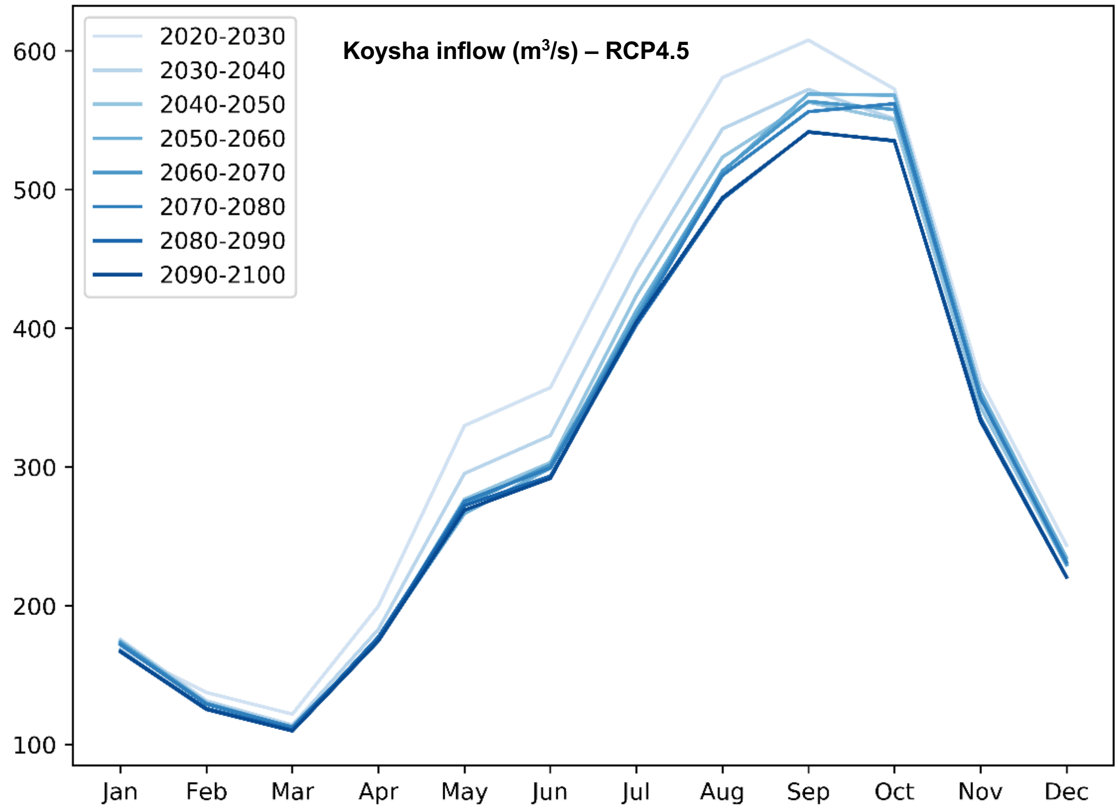

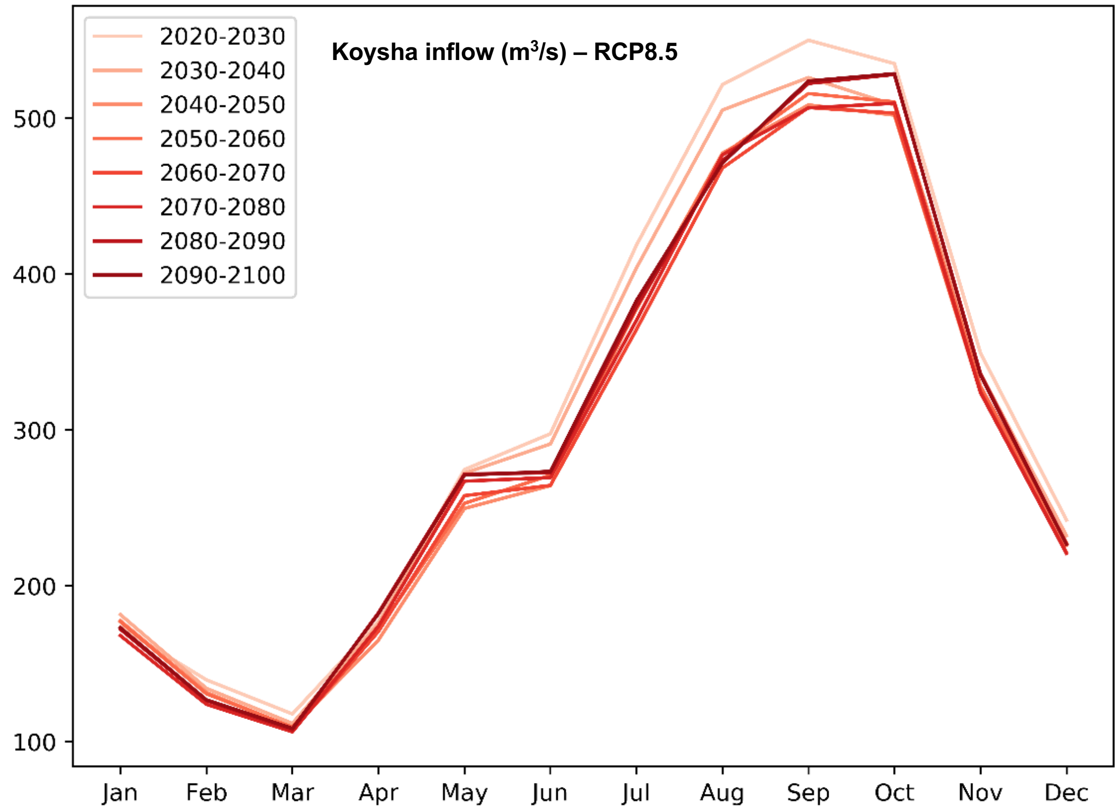

Figure 9 – Seasonal streamflow distributions before Koysha (m3/s) for RCP4.5 and RCP8.5 climate forcings (North central Omo). RCP4.5 shows a trend towards lower flows at the end of the century consistent with the relatively small change in precipitation relative to the increase in potential evaporation between present and end of century climate – the greater increase in evaporation for RCP8.5 results in generally lower streamflow compared with RCP4.5, however the trend for RCP8.5 shows mixed behaviour (see Figure 6 and Figure 7).

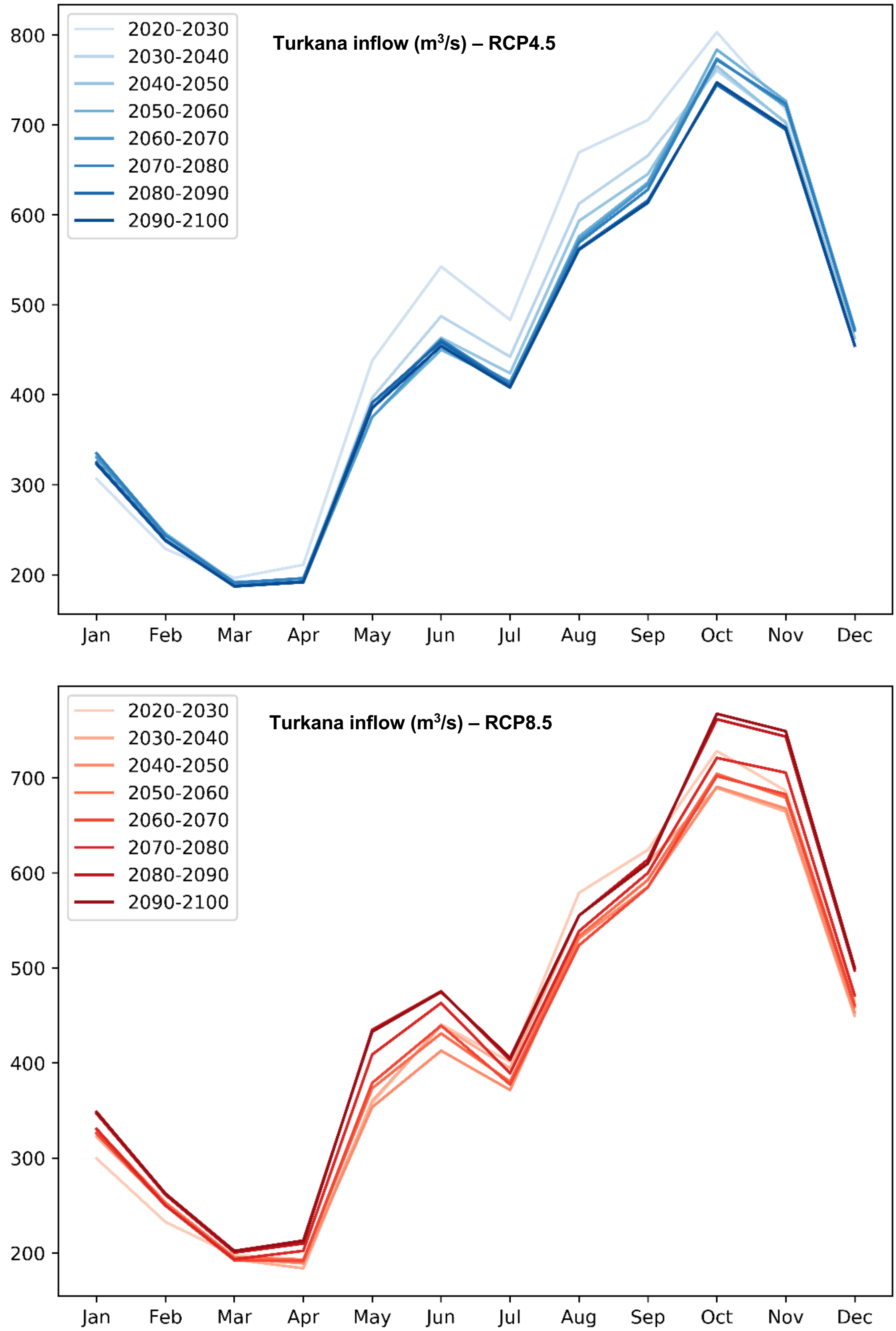

Figure 10 – Seasonal flow at Lake Turkana (m3/s) for RCP4.5 and RCP8.5 climate forcings (lower Omo). RCP4.5 shows a trend towards lower flows at the end of the century consistent with the small change in precipitation relative to the increase in potential evaporation between present and end of century climate –RCP8.5 shows generally lower streamflow compared with RCP4.5, however the trend for RCP8.5 shows an increase in streamflow towards the end of the century. The trend towards increasing flow for RCP8.5 is consistent with the relatively greater precipitation in the central and lower Omo compared to the increase in PET (see Figure 6 and Figure 7).

4.2 IRRIGATION DEMAND SCENARIOS

As in the case of the ZRB, also for the OTB irrigation future nominal scenarios were generated by using the AquaCrop model considering existing and planned irrigation schemes, the projected precipitation and temperature under RCP 4.5 as inputs, the soil characteristics from ISRIC[2] soil grids, default crop parameters, and assuming a 45% and a 58% irrigation efficiency. More details on the methodology can be found in Deliverable D2.2. The irrigation scenarios that will be simulated in the DAF consider the water demand associated with the Kuraz Sugar Development project, by far the largest and most water intensive irrigation scheme in OTB, extending for a total of 100 thousand hectares in a relatively dry region of the basin.

In addition to the 2 nominal scenarios, 8 synthetic scenarios were generated by perturbing the nominal scenarios of a fixed percentage, namely ±5% and ±10%, thus creating positive and negative deviations with respect to the nominal water demand allowing to assess the system performance for a wider range of irrigation abstractions. By exploring a range of values in the proximity of the nominal values, moreover, we account for possible errors introduced in the nominal estimations, e.g., due the irrigation model, input data, and assumptions.

The generated synthetic scenarios are reported in Figure 11 as a cyclostationary mean for the period 2020-2099, showing the irrigation demand is highest during the dry season, from January to April, and peaks in February, but relatively high demand is also reported in the months of July and August. The altered generated scenarios, represented by the boundaries of the shaded areas, allow to expand the analysis by accounting for lower, higher, and intermediate values with respect to the two nominal estimations. Figure 12 reports the average daily irrigation water demand under nominal (stars, bold) and synthetic (circles) scenarios: the generated scenarios appear well distributed across the vertical axis of water demands indicating a good characterization of the variable and its uncertainty.

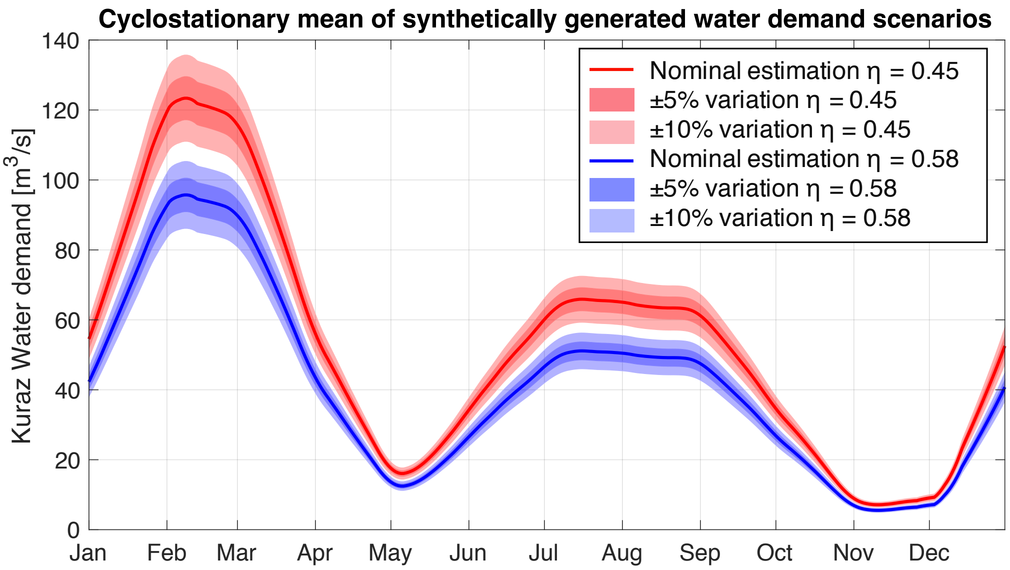

Figure 11 – Synthetic generation of water demand scenarios. Bold lines represent the cyclostationary mean of the estimated future water demands for the period 2020-2099 of Kuraz Sugar plantation for nominal efficiencies of 0.45 and 0.58 (red and blue line, respectively). The estimated water demand accounts for crop needs, evaporation, and precipitation, is highest during the dry season, from January to April, and peaks in February. The shaded areas correspond to the scenarios synthetically generated by perturbing the nominal demands of ±5% (darker shade) and ±10% (lighter shade), producing a total of 8 synthetically generated scenarios on top of the 2 nominal estimations.

[2] www.soilgrids.com

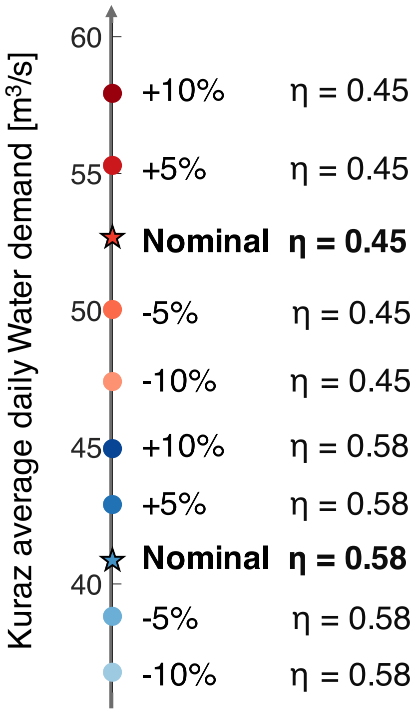

Figure 12 – A 1-dimensional exposure space reporting the mean daily water demands estimated for the future period 2020-2099 for the two nominal scenarios and the 8 synthetically generated scenarios corresponding to 0.45 and 0.58 efficiencies (red and blue points respectively). Overall, the generated scenarios span a range of values from a daily average of 36 m3/s for the most conservative scenario ($\eta = 0.58$ with a -10% perturbation) to 58 m3/s for the most water intensive scenario ($\eta = 0.45$ with a +10% perturbation)

5. CONCLUDING REMARKS

The data generated to characterise the exposure space summarised in this report will be the basis for the analysis of efficient and robust adaptation pathways, which will be described in D5.4. The indicator threshold that can provide the boundaries of acceptable system performance were preliminarily discussed at the second NSL held in July 2019 in the respective regions of the two case studies. As the discussion at the NSL showed, there is still need for additional debate about the acceptable system performance, so that we don't report here about more details about the indicator thresholds. These are implicitly reflected, however, by the deviations of the irrigation demands from the nominal ones, as these deviations correspond to forcing the irrigation demand to the highest values (e.g. low efficiency) or to keep the productivity required by the future food demand as identified in D2.2 but improving the irrigation management (e.g. higher efficiency).

6. REFERENCES

Allen, R., Pereira, L., Raes, D. and Smith, M. Crop evapotranspiration (1998) Guidelines for computing crop water requirements, FAO Irrigation and drainage paper 56.

Herman, J.D., Zeff, H.B., Reed, P.M. and G.W. Characklis (2014), Beyond optimality: Multistakeholder robustness tradeoffs for regional water portfolio planning under deep uncertainty, *Water Resour. Res.*, 50(10):7692–7713

Herman, J.D., Reed, P.M., Zeff, H.B. and G.W. Characklis (2015) How Should Robustness Be Defined for Water Systems Planning under Change, *Journal of Water Resources Planning and Management*, doi:10.1061/(ASCE)WR.1943-5452.0000509

Kasprzyk J.R., Nataraj S., Reed P.M., and R.J. Lempert (2013) Many objective robust decision making for complex environmental systems undergoing change, *Environ. Modell. Softw.*, 42, 55–71.

Lempert R.J., (2002) A new decision sciences for complex systems, *Proc. Natl. Acad. Sci.*, vol. 99, 7309–7313 Quinn J.D., Reed P.M., Giuliani M., Castelletti A., Oyler J.W. and R.E. Nicholas (2018) Exploring how changing monsoonal dynamics and human pressures challenge multireservoir management for flood protection, hydropower production, and agricultural water supply, *Water Resources Research*, 54.